Water Droplet Impact Energy Harvesting with P(VDF-TrFE) Piezoelectric Cantilevers on Stainless Steel Substrates

Samuel C. J. Jellard[1,2], Suan Hui Pu[3], Shuting Chen[2], Kui Yao[2], Neil M. White[1]

[1] Smart Electronic Materials and Systems Research Group, Electronics and Computer Science, University of Southampton, Southampton, United Kingdom, SO17 1BJ
[2] Institute of Materials Research and Engineering, A*STAR (Agency for Science, Technology and Research), 2 Fusionopolis Way, Innovis, Singapore 138634
[3]Mechatronics Research Group, University of Southampton, Southampton, SO17 1BJ, U.K. and the University of Southampton Malaysia, 79200 Iskandar Puteri, Johor, Malaysia

E-mail: samcjjellard@gmail.com

Received xxxxxx
Accepted for publication xxxxxx
Published xxxxxx

Abstract

Harvesting energy from ambient environmental sources using piezoelectric transducers has seen a tremendous amount of interest from the scientific community in recent times. The practicality of energy scavenging technology looks set to see continued relevance, with decreasing power demands of electrical systems, such as Wireless Sensor Networks (WSN), allowing such technology to progressively act as an energy source to drive and sustain them independently. In light of this, there is a growing opportunity for piezoelectric materials to prolong, or even replace, battery powered sensor systems positioned in remote or difficult to reach areas. It has been demonstrated that falling water droplets of millimetric-scale diameter can impart forces of over a thousand times their resting weight upon surface impact. As such, the potential for utilising piezoelectric transducers to drive sensor systems, by converting the kinetic impact energy of falling water droplets into useful electrical energy, is investigated. The key parameters that affect the efficiency of energy transfer between incident water droplets and piezoelectric cantilever structures made of stainless steel foil coated with the lead-free piezoelectric material P(VDF-TrFE) are investigated. A peak power output of 28 nJ achieved from the impact of a 5.5 mm diameter droplet upon a single energy harvesting transducer illustrated that, for droplets of diameter 3.1 mm to 5.5 mm impacting from heights between 0.5 to 2.0 m, it is desirable to utilise piezoelectric transducer beams of bending stiffness in the range of 0.067 to 0.134 N/m in order to achieve good energy transfer efficiency. Although the active electrode area was constrained in order to maintain consistency between samples, reducing the peak energy output, the achieved results correspond to a 15.9 J/m^3 energy density, representing the significant energy transfer efficiency achievable through appropriate transducer mechanical tailoring to the excitation source.

Keywords: Piezoelectric, Energy Harvesting, Droplet, Smart Materials, Microelectromechanical Systems, Rain Water

1. Introduction

Falling water droplets have been demonstrated to impart forces of over a thousand times their resting weight upon impact [1] Tropical countries regularly receive a deluge of large rainfall droplets falling upon natural and man-made structures, representing an interesting opportunity for further investigation regarding kinetic to electrical energy harvesting. Such systems may have the potential to drive interesting applications such as smart city sensor technology.

Research into droplet impact energy harvesting has seen limited progress to-date, with the majority of investigations utilising commercially available sensors to analyse droplet impact mechanics [2]–[4]. A non-exhaustive review of investigations into water droplet impact energy harvesting by piezoelectric transducers is provided by Wong *et al* [5]. Whilst good insight has been produced from these analyses, using commercial sensors as the energy harvesting transducer limits the degree to which the transducers can be modified to efficiently harvest the droplet impact stimulus. Investigations into water droplet energy harvesting appear to have been initiated formally by Guigon *et al* in 2008, where both the theory and experimental work contributing to efficient mechanical energy harvesting were outlined in a two-part study [6], [7]. The initial theoretical investigation illustrated how the mechanical sizing of the structure optimises the transfer of deformation energy from the drop to the piezoelectric polymer, before investigating the structure conversion efficiency through surface contact electrode design. It was concluded that the piezoelectric transducer material must be very thin (μm scale), not be pre-stressed and be of a width slightly smaller than the maximum diameter of the impacting drop for efficient energy harvesting to take place. Additionally, it was considered optimal for the piezoelectric material to be entirely covered with conducting electrodes. Simulations demonstrated a theoretical energy output of 25 μJ and peak instantaneous power output of 12 mW from a "downpour" drop of 5 mm diameter [6].

The corresponding experimental study demonstrated how mono-stretched PVDF polymer bands of 10 cm length, 3 mm width and 25μm thickness demonstrated a peak power output of approximately 1 nJ electrical energy and 1 μW of instantaneous power from a single droplet impact. It was observed that the recovery of electrical energy was maximised when droplet impacts were slightly off-centre from the beam material [7]. It is noted that no hydrophobic encapsulation was administered to the bands, therefore the droplet impacts were treated as inelastic.

These findings were supported by research carried out by Vasileiou *et al*, which explored how a reduction in substrate area density and stiffness imparts immediate acceleration and intrinsic responsiveness to impacting droplets [8]. Although this research did not utilize piezoelectric materials, and as such did not consider the effect of the relevant parameters on power output, their findings demonstrated efficient energy conversion from droplet kinetic energy to substrate kinetic and strain energy when the sample had low area density, comparable stiffness to that of the water droplet's surface tension, and minimal damping.

The initial work of Guigon *et al* inspired a number of follow-up investigations. Ilyas and Swingler analysed the voltage output profiles produced from droplet impact upon commercially available sensors in detail, identifying two distinct phases in voltage and power output; log growth at the initial impact, before exponential decay occurring throughout the remainder of the impact event. It was demonstrated that the log growth stage significantly contributes to the overall power output of the device [2], [9].

Research conducted by Viola et al has investigated droplet energy output with commercially available piezoelectric sensors, in addition to testing cantilever beam, bridge and centralized floating diaphragm harvester configurations [10]. It was found that the cantilever beam harvester configuration achieved the best response to impacting droplets, with a commercial LDT1-028K MEAS piezoelectric sensor producing 17 V output from droplets dispensed from a height of 2 m.

The performance of piezoelectric energy harvesters in both simulated and actual rainfall was evaluated by Wong et al [11], [12]. A spray-type rain simulator was used to dispense a range of droplet diameters from a height of 2.5 m onto a Midé Volture^{TM} commercial piezoelectric sensor (model V25W), composed of two PZT layers of 46 mm length, 33 mm width and 0.6 mm overall thickness. With the PZT layers connected in series across a 15 kΩ load resistor, simulated rainfall rates of 33, 40, 62 and 99 mm/h for a period of 300 seconds produced total power outputs of 0.074 μW, 0.156 μW, 0.167 μW and 0.207 μW respectively. Furthermore, the testing of the piezoelectric sensor in three actual rainfall events of duration 250, 204 and 301 minutes produced total harvested energies of 155.6 μJ, 438.9 μJ and 2076 μJ respectively. The significantly long time scale required to capture these energies highlights the inefficiency of attempting to harvest energy directly from rainfall droplet impacts.

In this work, fundamental findings regarding droplet impact energy harvesting are advanced by investigating the key parameters dictating efficient energy transfer. In order to encourage higher electrical power output, the piezoelectric transducer's bending stiffness k_b and resonant frequency f_r are focused upon. COMSOL Multiphysics simulations exploring simplified droplet impact onto piezoelectric beams were carried out initially. This was followed by an experimental study utilising purpose-built samples consisting of piezoelectric P(VDF-TrFE) polymer deposited onto stainless steel foil substrate beams. Using these samples, a variety of droplet diameters are dispensed onto the transducer beam end from a range of heights in order to explore the effect of beam stiffness on energy transfer efficiency.

Finally, an investigation into the energy transfer efficiency depending on droplet impact frequency is carried out. Whilst it is rational to assume that driving an energy harvester at its resonant frequency will result in maximised power output, it is proposed elsewhere that, depending on the relation between the beam resonant frequency and the natural vibration frequency of the impacting droplet (illustrated in Equation 1, where T is the natural oscillation period of a droplet [13]), the reactive transducer movement to impact can synergistically, passively or destructively contribute towards the droplet kinetic energy after recoil from the substrate [8]. As such, this research seeks to validate the effect of impact frequency upon the energy transfer efficiency, as this has yet to be explicitly demonstrated elsewhere.

$$f_d = \frac{1}{T} = \frac{1}{\frac{\pi}{4}\sqrt{\frac{\rho D_0^3}{\sigma}}} \qquad (1)$$

It has been reliably demonstrated that droplet-surface interactions are not trivial, given the elastic nature of droplets upon impact. Substrate flexibility directly affects the droplet impact behaviour, with "softer" substrates suppressing droplet splashing [14]. It is possible to achieve a two-fold reduction in contact time during a droplet impact if the superhydrophobic substrate is tailored to an appropriate elasticity, directly influencing the transfer of energy from the droplet to the transducer [15]. Correspondingly, the wettability of the sample surface directly influences the energy output achieved. Gart *et al* studied the effect of different surface treatments on the generated torque produced by elastic cantilever beams from droplet impact [16]. It was found that hydrophilic surfaces, which encourage water droplet adhesion after impact, led to greater bending energy being produced in the beam than beams where a hydrophobic surface treatment had been applied. This was due to the additional mass of the water droplet sticking to the cantilever during the impact process, subsequently generating a higher torque over time. It is proposed that, for a limited number of impacts, hydrophilic surface treatments are desirable – however, such surface treatments encourage the accumulation of water upon the energy harvesting surface, leading to excessive damping and loss of electrical energy output [17].

In this study, a superhydrophobic surface treatment will be utilised to isolate the piezoelectric beam. Although it has been demonstrated that hydrophobic treatments reduce the bending energy experienced by piezoelectric transducers, as the droplets tend to roll-off the harvester surface during impact, such treatments reduce the accumulation of water and increase the energy transfer efficiency of the harvesters in the long term. For reference, the contact angle of droplets upon a P(VDF-TrFE) layer without surface treatment is approximately 75° [18], increasing to above 160° with a superhydrophobic treatment, representing a significant decrease in surface wettability [19].

2. Sample Design Justification

Single-end clamped cantilever beams were selected as the test geometry, given the abundance of theoretical models which can be used to define and analyse such a system. The relationship expressing cantilever beam stiffness for a point load deflection applied at the free-end of the cantilever, perpendicular to the beam axis, is given in Equation 2. This relationship was used to describe the estimated stiffness of each test sample beam, where k_b is the beam bending stiffness, E is the beam elastic modulus, w is the beam width, t is the beam thickness and L is the beam length [20].

$$\mathrm{k_b} = \frac{\mathrm{Ewt^3}}{\mathrm{4L^3}} \qquad (2)$$

The relationship defining a cantilever beam's first order resonant frequency is shown in Equation 3, where E, t, ρ and L relate to the cantilever's Youngs modulus, thickness, density and length, respectively. The absence of a width term in this equation illustrates how the beam width can be varied in isolation to investigate the effect of beam stiffness variation on power output, without altering other mechanical parameters such as the beam's resonant frequency.

$$\mathrm{f_b} = \left(1.875^2\sqrt{\frac{\left(\frac{\mathrm{Et^2}}{12}\right)}{\rho \mathrm{L^4}}}\right) \cdot \frac{1}{2\pi} \qquad (3)$$

Following the guidance in the literature outlining the need for thin, responsive substrates in order to achieve efficient droplet energy harvesting, stainless steel foil of 25 μm thickness was used as a substrate, due to the material's inherent robustness, corrosion resistance and flexibility at thin gauges. P(VDF-TrFE) was selected for usage as the piezoelectric polymer also due to its flexibility. Considering the thickness weighted material properties of both the substrate and the P(VDF-TrFE) layer, it was calculated that a P(VDF-TrFE) layer of approximately 7.2 μm in thickness would position the beam's neutral axis to encourage an optimal piezoelectric voltage response, through facilitation of an advantageous bending regime [21]. In practice, it was found that such a thin layer of P(VDF-TrFE) on the selected stainless steel foil frequently resulted in breakdown during the poling process, so P(VDF-TrFE) layers of approximately 15 μm were fabricated.

3. Numerical Simulation of Stiffness Variation

Numerical simulation was carried out using COMSOL Multiphysics® Modeling Software. The in-built library materials "Steel AISI 4340" and "Polyvinylidene fluoride (PVDF)" were used to simulate the foil substrate and piezoelectric layer respectively. The properties of these materials are tabulated in Table I.

Beams of length 43 mm were simulated, with one end being held under fixed constraint. At the other end, a pulsed load was applied using a circular work plane parallel to the beam's upper surface to represent the impact of a droplet. The work plane diameter was simulated at 3.1 mm, 4.4 mm and 5.5 mm dimensions to represent the droplet diameter variations achievable from the range of experimental syringe nozzle outlets available.

TABLE I
SIMULATION MATERIAL PROPERTIES

Parameter	Value
Youngs Modulus Steel AISI 4340	205 GPa
Poisson's ratio of Steel AISI 4340	0.28
Density of Steel AISI 4340	7850 kg/ m^3
Youngs Modulus Polyvinylidene fluoride (PVDF)	3 GPa
Poisson's ratio of Polyvinylidene fluoride (PVDF)	0.18
Density of Polyvinylidene fluoride (PVDF)	1780 kg/ m^3
Polyvinylidene fluoride (PVDF) Piezoelectric Strain Constant d_{31} (shear mode direction 1)	13.6 pC/N
Polyvinylidene fluoride (PVDF) Piezoelectric Strain Constant d_{33} (thickness mode direction 3)	29.7 pC/N

The impact force for each diameter droplet was calculated using Equation 4, which estimates the impact force as a dynamic pressure $\rho_{water}\, v^2$ applied over a surface area of πr^2 [1]. This force was then translated into a force per unit area, and applied as a boundary load to the work plane. The speed of the droplet upon impact is assumed to be terminal velocity, and is calculated using Equation 5, where ρ_{water} is the water density (1000 kg/m^3), ρ_{air} is air density (1.225 kg/m^3) and C_d is the drag coefficient for a sphere (0.47). The duration of this impact or "crash time" was calculated using Equation 6 [15], where τ is the crash time, D_o is the droplet diameter before impact and v is the droplet's impact speed, assumed to be the droplet's terminal velocity here.

$$F_0 = \pi \rho_{water}\, r^2 v^2 \tag{4}$$

$$v_t = \left(\frac{8\rho_{water} r g}{3\rho_{air} C_d}\right)^{1/2} \tag{5}$$

$$\tau = \frac{D_o}{v} \tag{6}$$

An additional rectangular work plane of dimensions 22 mm length, 2 mm width was drawn on the upper surface of the beam to represent an upper contact electrode. An output load impedance sweep determined that the design was electrically impedance matched at 50 MΩ. The simulation time study period was 0.1 seconds, which ensured that the initial impact and subsequent initial beam displacement were captured. The simulation setup is illustrated in Fig. 1. The beam width was varied from 4 mm to 24 mm for each droplet diameter, with the power output results for each of the 3 droplet diameters tested illustrated in Fig. 2. The power output magnitude is over-estimated due to both the ideal behaviour of the simulated material, in addition to the sharp-impulse load duration used to represent non-trivial droplet impact dynamics.

Despite the difference in power output between simulated and fabricated devices, the result trend indicating that beams with lower bending stiffness generate greater output power proves valid.

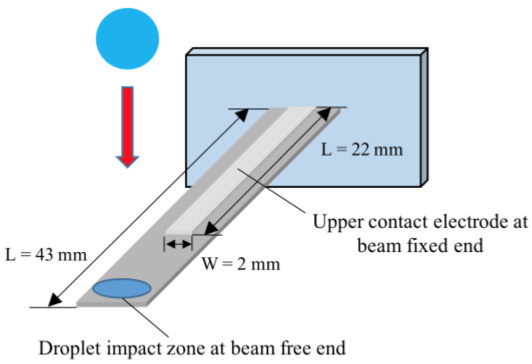

Fig. 1. Illustration of numerical model geometry setup simulating water droplet impact upon cantilever beam end

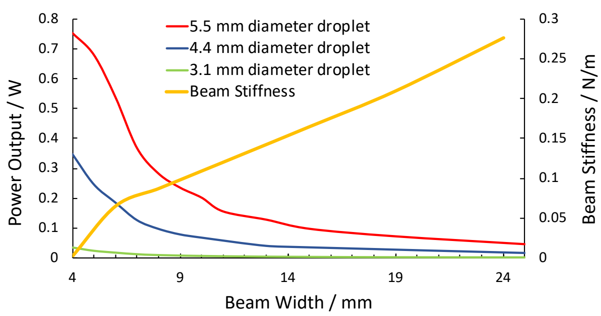

Fig. 2. Simulated effect of beam stiffness variation on peak power output from droplet impacts at terminal velocity.

4. Fabrication and testing of P(VDF-TrFE) on stainless steel foil cantilever beams

4.1 Sample Fabrication

A solution was prepared by dissolving 20% weight P(VDF-TrFE) co-polymer powder (70/30 mol ratio) in a solvent of dimethylformamide and acetone (volume ratio 20/80). The solution was heated at 55°C in an oil bath and mechanically stirred for approximately 1 hour, before being degassed in an ultrasonic water bath for 1-2 hours.

A micrometer adjustable applicator was used to uniformly spread the P(VDF-TrFE) solution on a stainless steel foil sheet. To accommodate for shrinkage during the annealing process, the applicator was set to produce 25 µm film thickness in order to achieve a final 15 µm film thickness post heat treatment. After depositing, the sheet was placed in an oven at 100°C for 5 minutes to allow the solution to dry. The sheet was then annealed for 2 hours at a temperature of 135°C in order to increase the piezoelectric material's crystallinity.

Following the heat treatment, the sheet was poled using a corona poling rig for 10 minutes at poling voltage of ~18 kV, before being cut into 6 samples of uniform length and thickness, but with varying widths of 6, 8, 10, 24, 26 and 27 mm. In this instance, lengths of 63 mm were selected in order to achieve low sample resonant frequencies (~10 Hz), allowing for 20 mm of beam length for clamping and electrode connections. Relevant sample properties are given in Table II.

Silver electrodes of approximately 32 mm length, 2 mm width, and 200 nm thickness were deposited through a shadow mask via e-beam evaporation. Wire connections were attached to the deposited electrode using silver electrode paste, before each sample was clamped using acrylic beams of 10 mm width, at a position of 10 mm away from the electrode connections area of the beams, as illustrated in Fig. 3. Finally, the samples were encapsulated using NeverWet® superhydrophobic surface treatment in order to isolate all electrical connections from water.

It was noted that samples suffered from slight initial deformation in some cases, due to both increasing mass and a residual stress gradient arising from the fabrication process. To negate any bias to testing results, two separate experiments were conducted – one which studied a series of samples, and a second which investigated a single sample in order to ensure consistency in experimental setup.

TABLE II
LENGTH = 63 MM, THICKNESS = 40 µM SAMPLE EXPERIMENTAL VALUES

Sample Width / mm	Resonant Frequency / Hz	Electrically impedance matched load / MΩ	Measured beam stiffness / N/m
6	10	8	0.0943
8	10	8	0.1170
10	10	8	0.1290
24	11	5	0.3070
26	10	5	0.3067
27	10	8	0.3066

TABLE III
LENGTH = 63 MM, THICKNESS = 40 µM, PROGRESSIVE TRIM SAMPLE EXPERIMENTAL VALUES

Sample Width / mm	Resonant Frequency / Hz	Electrically impedance matched load / MΩ	Measured beam stiffness / N/m
4	10	8	0.067
7	10	8	0.094
11	10	8	0.134
15	10	8	0.188
19	10	8	0.188
25	10	8	0.235
27	10	8	0.235

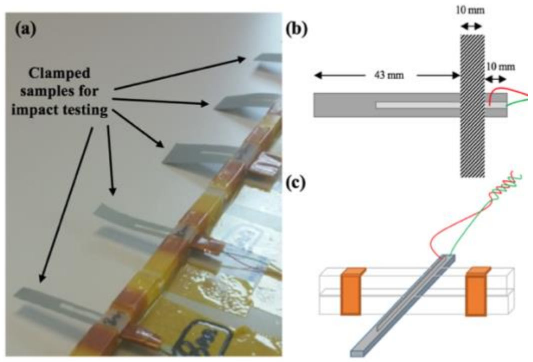

Fig. 3. Images to illustrate clamping set-up for 63 mm length samples. (a) depicts a photograph of samples used for testing. (b) illustrates sample dimensions - free beam length is 43 mm, with 10 mm being clamped securely with acrylic supports, and the last 10 mm of the beam reserved for electrode connections. (c) illustrates sample clamping set-up graphically.

4.2 Effect of beam stiffness variation on power output from droplet impact

The experimental test rig used to investigate beam stiffness variation is illustrated in Fig. 4. The rig consisted of an adjustable clamp, able to adjust to a height of approximately 2.4 m, a base stand and drip tray. Syringes placed in the clamp were used to dispense droplets of diameter 3.1 mm, 4.4 mm and 5.5 mm from different heights. Samples were fixed onto a single, solid acrylic board, which was positioned on top of the drip tray underneath the clamped syringe nozzle. The centroid location of droplet impact was no greater than 5 mm from the end of each beam's free end. The piezoelectric beam output was connected to an electrically impedance matched resistive load, with the generated voltage response across the resistor measured using an MDO3000 series Tektronix® Oscilloscope.

Two rounds of testing took place – the first measured the power output generated from the impact of the 3.1 mm, 4.4 mm and 5.5 mm diameter droplets dispensed from heights of 0.5 m, 1 m, 1.5 m and 2 m for each of the 6 samples. It was observed that larger samples tended to suffer initial displacement due to their increased mass. In order to validate that this did not detrimentally effect any result trend achieved, a second test round was carried out.

This test round focused on progressively trimming the width of the 27 mm wide sample in isolation, illustrated in Fig. 5, whilst impact testing with the same three different droplet diameters from heights of 0.5 m, 1 m and 1.5 m. Testing was carried out in this manner to ensure that any physical differences between samples were negated. Furthermore, sample characteristics, such as initial displacement, were kept constant between width alterations adding further control to the experiment. Testing multiple samples, however, demonstrated that the stiffness values achieved were not unique to the individual sample used in the progressive trim testing. The properties of the sample used at each interval during the progressive trim testing round are displayed in Table III.

4.3 Droplet impact frequency effect on power output

In order to test the effect of droplet impact frequency on power output, an Alaris IVAC P7000 syringe driver was used to dispense 3 mm-diameter droplets at a range of drip frequencies onto each sample beam end. This test round utilized the samples used in previous tests (widths of 4, 6, 8, 10, 24 and 26 mm). The properties of these samples are shown in Tables II and III. Fig. 5 presents the photos to illustrate progressive trim test sample modification. An IR detector was used to measure the drip frequency rate of the droplets, outputting a negative spike each time a droplet broke the IR beam, as shown in Fig. 6. This signal was measured using an oscilloscope and used to calculate drip frequency. Measured drip frequencies ranged from 1 Hz to at least 30 Hz for all samples.

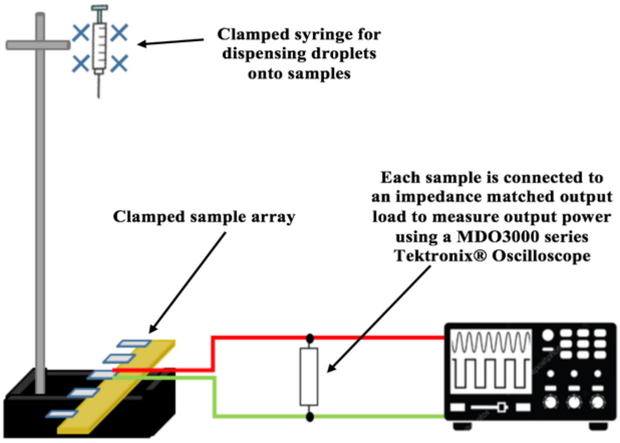

Fig. 4. Diagram to illustrate droplet impact test setup

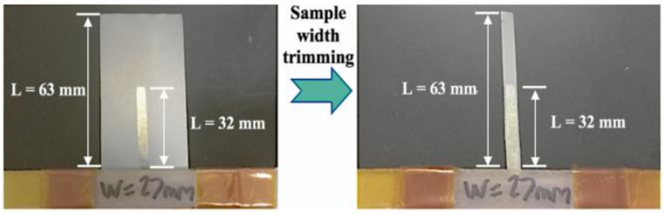

Fig. 5. Photo to illustrate progressive trim test sample modification

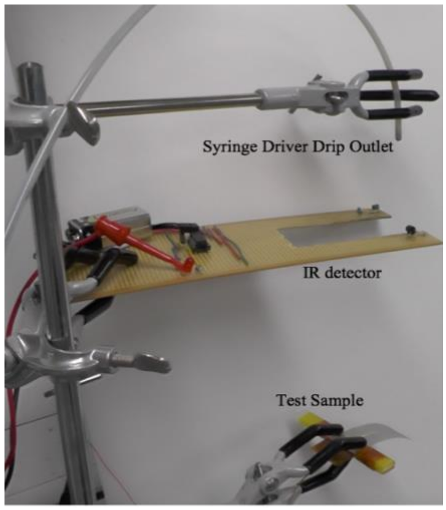

Fig. 6. Photograph to illustrate droplet impact frequency effect on power output test setup

5. Results and Discussion

5.1 Effect of beam stiffness variation on power output – multiple samples results

The results in Fig. 7 show that beams with bending stiffness in the region of 0.1 N/m are better for droplet energy harvesting. The output energy per impact produced by the beam with 8 mm width (bending stiffness of 0.1170 N/m) produced the highest output energy levels throughout a range of different diameter droplet impacts, peaking at an output of 28 nJ for a single 5.5 mm diameter droplet impact from a release height of 1.5 m. Fig. 8 displays the averaged energy outputs of all release heights for each droplet diameter tested, in order to highlight the peak energy output achieved by the 8 mm width beam for each droplet diameter.

5.2 Effect of beam stiffness variation on power output – progressive trim testing of single 27 mm width sample results

When a single sample had its stiffness modified in the case of the progressive trim tests, the results illustrated in Fig. 9 again demonstrate that beams with bending stiffness of approximately 0.1 N/m are better for droplet harvesting, with the beam of width 7 mm, bending stiffness 0.094 N/m, producing the highest energy output levels per impact for the range of droplet diameters and release heights tested. The peak output power for the 7 mm beam undergoing single droplet impact was 14 nJ, generated by a 5.5 mm diameter droplet falling from a release height of 1.5 m. Fig. 10 displays the averaged energy outputs of all release heights for each droplet diameter tested, in order to highlight the peak energy output achieved by the 7 mm width beam for each droplet diameter.

5.3 Droplet impact frequency effect on power output results

The impact frequency testing results in Fig. 11 indicate that, despite the non-trivial behaviour of droplet-surface impact interactions, sample output power was better when the frequency of incident impacting droplets onto the sample beam ends' was close to/at the samples resonant frequency. It was noted that the simulated power output levels were a couple of magnitudes greater than the practical results. It is proposed that this is due to the simplified loading condition used in the simulation environment, which neglects the complex fluid-structure interaction of droplet impact in reality. Nonetheless, these results support the conclusion that driving the samples at their resonant frequency achieves optimal power output. The slight difference in power output peaks between the simulated and practical results are likely due to mechanical imperfections in the experimental sample set.

This is considered to be due to the disparities between the simulation and experimental materials, which will likely differ due to real-world processing requirements. In each case, the power output was maximised when the simulated/practical sample was driven by impacts matching its resonant frequency.

5.4 Result Analysis & Discussion

Previous research carried out in the area of droplet energy harvesting using piezoelectric materials has found that the energy transfer efficiency of such systems is typically very low, in the order of approximately 0.12% [2]. This figure was achieved using a commercially available piezoelectric sensor, the Pro-Wave (FS-2513P). Although the theoretical energy transfer efficiency of the results reported here was approximately 0.0013%, representing the ideal energy available from a 5.5 mm diameter droplet falling from 1.5 m as 1.28 mJ, it is important to consider that the electrode area was constrained in order to retain experimental consistency as beam width variation was carried out.

Furthermore, a comparison of transducer energy densities highlights the benefits of mechanical tailoring to the excitation source. The results from the cited literature utilising the commercial Pro-Wave (FS-2513P) sensor [2] indicate an energy output of no more than 90 nJ from droplet impact. With an active volume of approximately 0.975 μm^3, the energy density is calculated as 0.092 J/m^3. In comparison, the peak energy output of 28 nJ achieved here, across an active sample volume of 1.76 nm^3, represents an energy density of 15.9 J/m^3.

As such, whilst the peak energy output achieved in this research is not the highest possible, it demonstrates significant energy transfer efficiency for the active electrode areas used. It is proposed that the energy density of the commercial sensors typically utilised in other studies is notably lower due to the relatively stiff Mylar coating used to encapsulate the sample. Furthermore, with the sample clamped in a cantilever beam orientation, the impact zone of the droplet upon the transducer was targeted at the beam center, instead of the beam end. This would have increased the transducer's apparent stiffness to the droplet impact, decreasing the responsiveness of the beam and resulting in further degradation of the energy transfer efficiency. The simulation and experimental results of this study indicate that both low beam stiffness in the region of 0.1 N/m, in addition to transducer resonant frequency being close to/at the driving frequency of the energy source, are required for efficient energy transfer to occur between the impacting droplet and the piezoelectric transducer.

Furthermore, the results illustrate that a relatively small variation in beam width, relating to a consequent change in bending stiffness, can significantly affect the energy transfer efficiency. For example, when impacting a 3.1 mm diameter droplet from 0.5 m onto the progressive trim test sample, an energy output of 5.1 nJ was achieved with a 7 mm width beam, compared to a 1 nJ output obtained from the beam at 27 mm width. This represents an approximate 5-times increase in energy transfer efficiency, in relation to a variation of 20 mm in sample width, underlining the importance of transducer parameter tailoring depending on the expected droplet size and impact speed.

Similarly, in situations where continuous droplet impact is expected, the results achieved here underline the corresponding importance of transducer resonant frequency matching. For example, the sample of width 8 mm produced approximately 3.6 nW peak output power when driven with droplets at a frequency of 1 Hz. However, when driven with droplets at its resonant frequency of 10 Hz, a peak output power of 12 nW was achieved, representing a 4-time increase in output power.

Given the significant effect of such parameter tailoring on energy transfer efficiency, should energy harvesting from rainfall be a target application, the results suggest that greater energy efficiency can be achieved through accumulating the rainfall in a storage tank initially, before dispensing droplets using a tiered outlet system. This would serve to control the droplet size and impact frequency, in order to better match the key transducer parameters outlined in this report, resulting in much greater power output than perhaps otherwise achievable through attempting to harvest energy from direct rainfall impact. Should a sufficient amount of water be accumulated, an array of energy harvesting devices fabricated using the design guidelines outlined in this research could drive low power systems by storing and supplying the accumulated energy via an efficient energy management system, such as an ultra-sharp transistor based switching circuit [22]. For example, such energy could be used to drive medium to short range wireless sensor applications, utilising components such as Microsemi's ZL70550 RF transceiver [23] supported by an ultra-low power management IC such as the S6AE10xA energy harvesting PMIC from Cypress Semiconductor [24].

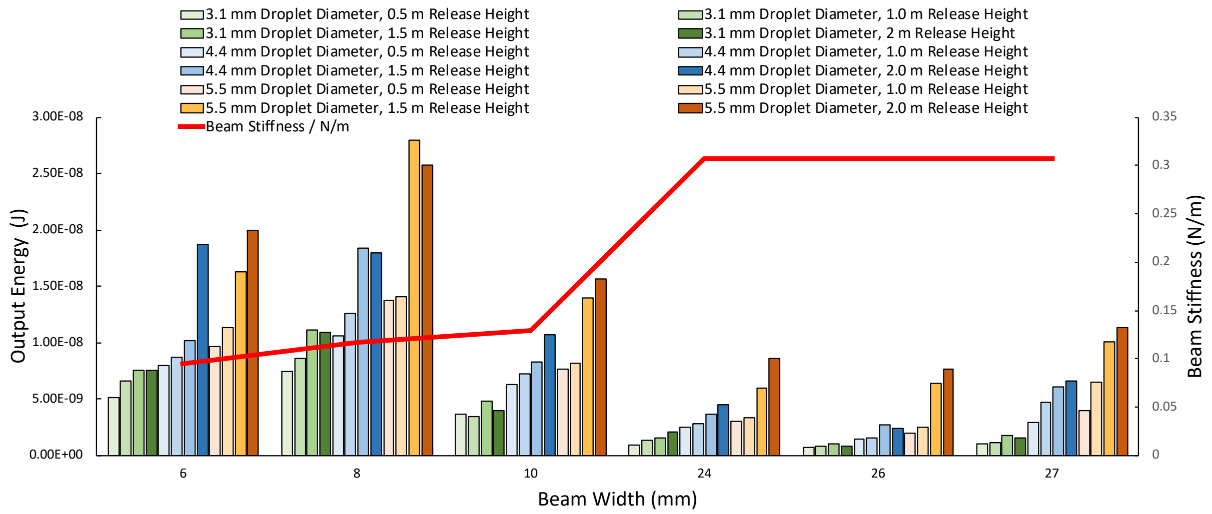

Fig. 7. Average output energy per beam width as a function of impacting droplet diameter and release height, multiple test samples

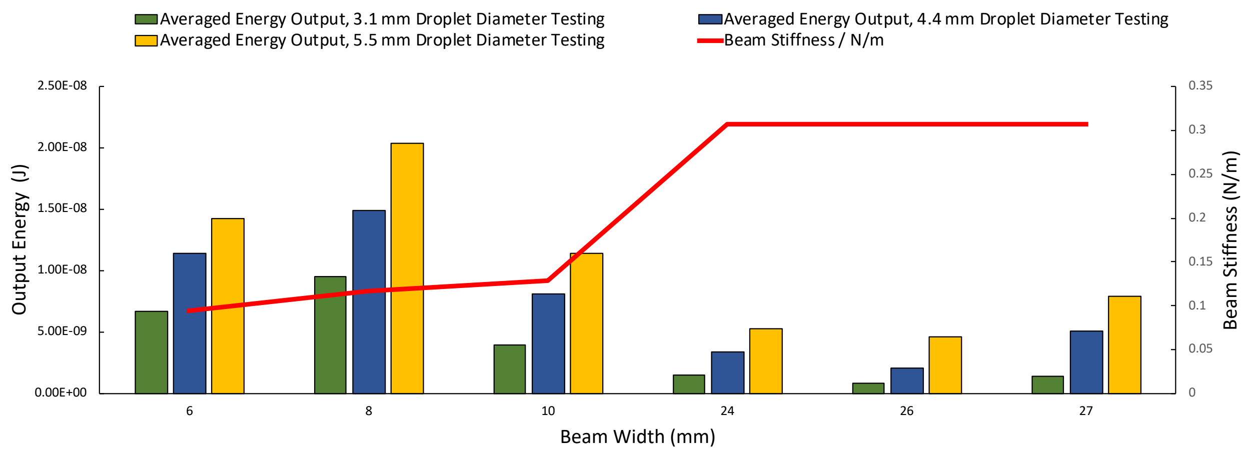

Fig. 8. Graph displaying all droplet release height results from Fig. 7. (multiple test samples) averaged to give a single output energy, per beam width, for each droplet diameter tested

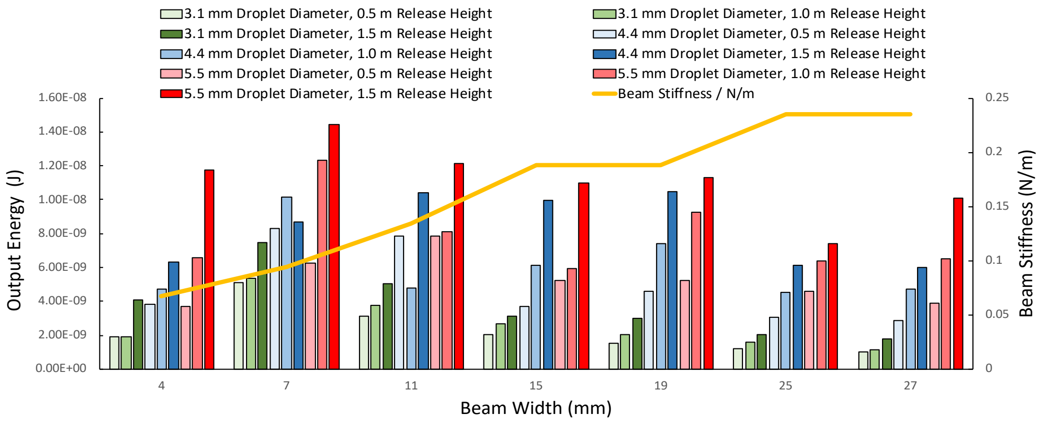

Fig. 9. Average output energy per beam width as a function of impacting droplet diameter and release height, progressive trim testing

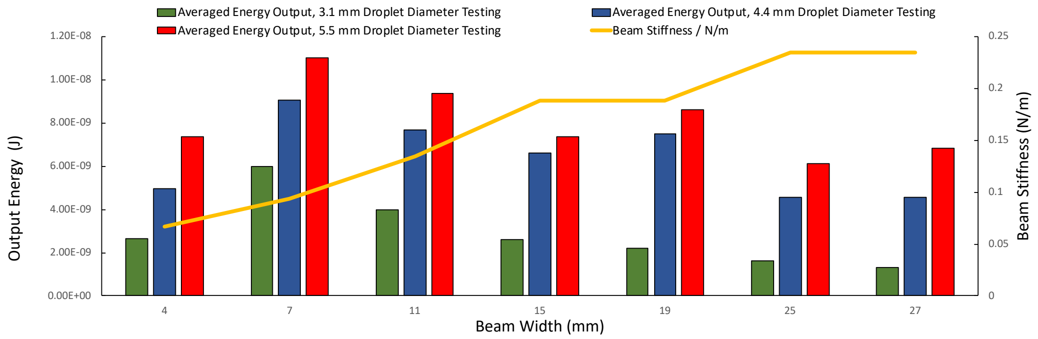

Fig. 10. Graph displaying all droplet release height results from Fig. 9 (progressive trim testing) averaged to give a single output energy, per beam width, for each droplet diameter tested

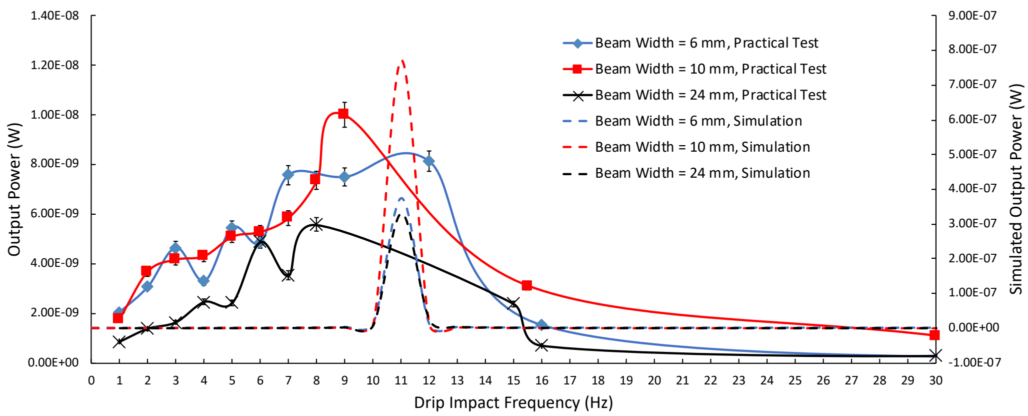

Fig. 11. Sample output power as a function of droplet impact frequency

6. Conclusion

In this paper, we investigated the key parameters that affect the efficiency of energy transfer between incident water droplets and piezoelectric cantilever structures made of stainless steel foil coated with piezoelectric P(VDF-TrFE). The experimental results and analyses achieved underlined the importance of appropriate transducer stiffness and resonant frequency matching, depending on the expected impact behaviour of incident droplets. The resulting enhancement in power output was demonstrated to be of magnitude scale with optimal piezoelectric transducer stiffness and resonance frequency matching.

From the results of both impact tests, it was demonstrated that for droplets of diameter 3.1 mm to 5.5 mm, impacting from heights between 0.5 to 2.0 m, it is desirable to utilise piezoelectric transducer beams of bending stiffness in the range of 0.067 to 0.134 N/m in order to achieve good energy transfer efficiency, resulting in enhanced electrical power output. Additionally, it was found that the power output was further increased when the impact frequency was close to/at the transducers resonant frequency. Our investigation results provide valuable guidelines for piezoelectric transducer design for effective mechanical energy harvesting from rain droplets.

Acknowledgements

S. C. J. Jellard would like to sincerely thank the IMRE lab staff for their support and guidance throughout this research, in particular Dr. Weng Heng Liew, Dr. Meysam Sharifzadeh Mirshekarloo and Dr. Lei Zhang. The authors at IMRE acknowledge the partial support by Singapore Maritime Institute under the Maritime Sustainability R&D Programme, Project ID: SMI-2015-MA-07 (IMRE/16-7P1125). S. C. J. Jellard would also like to thank the University of Southampton's Faculty of Engineering and Physical Sciences for the Tizard studentship and A*STAR for the ARAP Scholarship.

References

[1] D. Soto, A. B. De Larivière, X. Boutillon, C. Clanet, and D. Quéré, "The force of impacting rain," *Soft Matter*, vol. 10, no. 27, pp. 4929–4934, 2014.

[2] M. A. Ilyas and J. Swingler, "Piezoelectric energy harvesting from raindrop impacts," *Energy*, vol. 90, pp. 796–806, 2015.

[3] D. Vatansever, R. L. Hadimani, T. Shah, and E. Siores, "An investigation of energy harvesting from renewable sources with PVDF and PZT," *Smart Mater. Struct.*, vol. 20, no. 5, p. 055019, 2011.

[4] F. Viola, P. Romano, R. Miceli, and G. Acciari, "On the harvest of rainfall energy by means of piezoelectric transducer," *Proc. 2013 Int. Conf. Renew. Energy Res. Appl. ICRERA 2013*, no. October, pp. 1133–1138, 2013.

[5] C. H. Wong, Z. Dahari, A. Abd Manaf, and M. A. Miskam, "Harvesting raindrop energy with piezoelectrics: A review," *J. Electron. Mater.*, vol. 44, no. 1, pp. 13–21, 2015.

[6] R. Guigon, J.-J. Chaillout, T. Jager, and G. Despesse, "Harvesting raindrop energy: theory," *Smart Mater. Struct.*, vol. 17, no. 1, p. 015038, 2008.

[7] R. Guigon, J. Chaillout, and T. Jager, "Harvesting raindrop energy : experimental study," *Smart Mater. Struct.*, vol. 17, no. 1, p. 015039, 2008.

[8] T. Vasileiou, J. Gerber, J. Prautzsch, T. M. Schutzius, and D. Poulikakos, "Superhydrophobicity enhancement through substrate flexibility," *Proc. Natl. Acad. Sci.*, vol. 113, no. 47, pp. 13307–13312, 2016.

[9] M. A. Ilyas and J. Swingler, "Towards a prototype module for piezoelectric energy harvesting from raindrop impacts," *Energy*, vol. 125, pp. 716–725, 2017.

[10] F. Viola, "Comparison Among Different Rainfall Energy Harvesting Structures," *Appl. Sci.*, vol. 8, no. 6, p. 955, 2018.

[11] V. Wong, J. Ho, E. H. Yap, and A. B. Chai, "Dynamics of a piezoelectric energy harvester in a simulated rain environment," vol. 232, no. 15, pp. 2642–2654, 2018.

[12] V. Wong, J. Ho, and A. Chai, "Performance of a piezoelectric energy harvester in actual rain," *Energy*, vol. 124, pp. 364–371, 2017.

[13] H. Lamb, *Surface Waves*, vol. 26. Cambridge University Press, 1895.

[14] R. E. Pepper, L. Courbin, and H. A. Stone, "Splashing on elastic membranes: The importance of early-time dynamics," *Phys. Fluids*, vol. 20, no. 8, 2008.

[15] P. B. Weisensee, J. Tian, N. Miljkovic, and W. P. King, "Water droplet impact on elastic superhydrophobic surfaces," *Sci. Rep.*, vol. 6, no. July, p. 30328, 2016.

[16] S. Gart, J. E. Mates, C. M. Megaridis, and S. Jung, "Droplet Impacting a Cantilever: A Leaf-Raindrop System," *Phys. Rev. Appl.*, vol. 3, no. 4, pp. 1–8, 2015.

[17] V. K. Wong, J. H. Ho, and H. K. Sam, "On accumulation of water droplets in piezoelectric energy harvesting," *J. Intell. Mater. Syst. Struct.*, vol. 28, no. 4, pp. 521–530, 2017.

[18] G. E. Crippa, R. Gimenes, M. A. Zaghete, and P. T. De Oliveira, "Response of human alveolar bone-derived cells to a novel poly (vinylidene fluoride-trifluoroethylene)/ barium titanate membrane Response of human alveolar bone-derived cells to a novel poly (vinylidene fluoride-trifluoroethylene)/ barium titanate memb," *J. Mater. Sci. Mater. Med.*, no. February 2017, 2011.

[19] NeverWet LLC, "Product Characteristics," *NeverWet*, 2016. [Online]. Available: https://www.neverwet.com/applications/product-characteristics.php. [Accessed: 15-Apr-2019].

[20] J. M. Gere and S. P. Timoshenko, "Mechanics of Materials," *Mech. Mater.*, p. 913, 1997.

[21] L. Zhang, S. R. Oh, T. C. Wong, C. Y. Tan, and K. Yao, "Piezoelectric polymer multilayer on flexible substrate for energy harvesting," *IEEE Trans. Ultrason. Ferroelectr. Freq. Control*, vol. 60, no. 9, pp. 2013–2020, 2013.

[22] S. C. Lai, K. Yao, and C. Y. Tan, "A Battery-less Sensor Concept Outputting Perceivable Signal Demonstrated with an Accelerometer," *IEEE Sensors*, pp. 1–6, 2016.

[23] "ZL70550 Ultra-Low-Power Sub-GHz RF Transceiver (779 MHz to 965 MHz)," Microsemi, 2019. [Online]. Available: https://www.microsemi.com/product-directory/sub-ghz-radio-transceivers/3928-zl70550.

[24] "Cypress Semiconductor Corp CYALKIT-E03," Cypress Semicond. Corp, 2019. [Online]. Available: https://www.digikey.co.uk/products/en/development-boards-kits-programmers/evaluation-boards-expansion-boards-daughter-cards/797?k=CYAL